4. K. V. Kuchibhotla *et al.*, *Neuron* **59**, 214 (2008).
5. X. Wang *et al.*, *Nat. Neurosci.* **9**, 816 (2006).
6. J. Schummers, H. Yu, M. Sur, *Science* **320**, 1638 (2008).
7. H. Hirase, L. Qian, P. Bartho, G. Buzsaki, *PLoS Biol.* **2**, E96 (2004).
8. N. J. Maragakis, J. D. Rothstein, *Nat. Clin. Pract. Neurol.* **2**, 679 (2006).
9. J. Wegiel *et al.*, *Neurobiol. Aging* **22**, 49 (2001).
10. T. Wyss-Coray *et al.*, *Nat. Med.* **9**, 453 (2003).
11. T. Takano, X. Han, R. Deane, B. Zlokovic, M. Nedergaard, *Ann. N. Y. Acad. Sci.* **1097**, 40 (2007).
12. C. D. Wilms, H. Schmidt, J. Eilers, *Cell Calcium* **40**, 73 (2006).
13. M. Garcia-Alloza *et al.*, *Neurobiol. Dis.* **24**, 516 (2006).
14. D. R. Borchelt *et al.*, *Neuron* **19**, 939 (1997).
15. C. Agulhon *et al.*, *Neuron* **59**, 932 (2008).
16. E. Scemes, C. Giaume, *Glia* **54**, 716 (2006).
17. A. H. Cornell-Bell, S. M. Finkbeiner, M. S. Cooper, S. J. Smith, *Science* **247**, 470 (1990).
18. T. A. Fiacco, K. D. McCarthy, *Glia* **54**, 676 (2006).
19. S. Boitano, E. R. Dirksen, M. J. Sanderson, *Science* **258**, 292 (1992).
20. M. L. Cotrina, J. H. Lin, J. C. Lopez-Garcia, C. C. Naus, M. Nedergaard, *J. Neurosci.* **20**, 2835 (2000).
21. P. B. Guthrie *et al.*, *J. Neurosci.* **19**, 520 (1999).
22. M. Garcia-Alloza, S. A. Dodwell, M. Meyer-Luehmann, B. T. Hyman, B. J. Bacskai, *J. Neuropathol. Exp. Neurol.* **65**, 1082 (2006).
23. A. Y. Abramov, L. Canevari, M. R. Duchen, *J. Neurosci.* **23**, 5088 (2003).
24. J. Petravicz, T. A. Fiacco, K. D. McCarthy, *J. Neurosci.* **28**, 4967 (2008).
25. We thank K. O. Ohki and R. C. Reid for assistance with the multicell bolus loading technique. This work was supported by NIH grants EB000768 (B.J.B.), AG08487 (B.T.H.), and NS580752 (K.V.K.).

Supporting Online Material

www.sciencemag.org/cgi/content/full/323/5918/1211/DC1
Materials and Methods
Figs. S1 to S6
Movies S1 and S2
References

27 November 2008; accepted 16 January 2009
10.1126/science.1169096

Meropenem-Clavulanate Is Effective Against Extensively Drug-Resistant *Mycobacterium tuberculosis*

Jean-Emmanuel Hugonnet,[1] Lee W. Tremblay,[1] Helena I. Boshoff,[2] Clifton E. Barry 3rd,[2] John S. Blanchard[1]*

β-lactam antibiotics are ineffective against *Mycobacterium tuberculosis*, being rapidly hydrolyzed by the chromosomally encoded *blaC* gene product. The carbapenem class of β-lactams are very poor substrates for BlaC, allowing us to determine the three-dimensional structure of the covalent BlaC-meropenem covalent complex at 1.8 angstrom resolution. When meropenem was combined with the β-lactamase inhibitor clavulanate, potent activity against laboratory strains of *M. tuberculosis* was observed [minimum inhibitory concentration ($MIC_{meropenem}$) less than 1 microgram per milliliter], and sterilization of aerobically grown cultures was observed within 14 days. In addition, this combination exhibited inhibitory activity against anaerobically grown cultures that mimic the "persistent" state and inhibited the growth of 13 extensively drug-resistant strains of *M. tuberculosis* at the same levels seen for drug-susceptible strains. Meropenem and clavulanate are Food and Drug Administration–approved drugs and could potentially be used to treat patients with currently untreatable disease.

Tuberculosis is perhaps the most persistent human disease caused by an infectious bacterium, *Mycobacterium tuberculosis*. The death toll remains extremely high, despite the introduction of modern multidrug chemotherapy in the 1960s, with between 1.6 and 2 million fatalities annually. An increasing percentage of human clinical isolates are drug-resistant or multidrug-resistant strains that threaten the ability to treat the disease (*1*). The continued use of multidrug therapy has caused an even more dire problem: strains of *M. tuberculosis* resistant to all first-, second-, and third-line agents. In a recent study from South Africa, 54 of 54 patients infected with such highly resistant strains died with a mean survival time from diagnosis of 16 days (*2*).

Since the discovery of penicillin in 1929 (*3*), the β-lactam class of antibiotics has included some of the most clinically important antibacterial agents. The development of broad-spectrum derivatives of penicillin, such as the cephalosporins and olivanic acid (*4*), coupled with their low inherent toxicity have made them the drugs of choice for the treatment of both Gram-negative and Gram-positive bacterial infections. This class, however, has never provided a compound useful in the treatment of tuberculosis, and β-lactams are only rarely used in the treatment of this disease. One important reason for the lack of efficacy was found in the genome sequence of *M. tuberculosis*, which contains a single, highly active, chromosomally encoded class A (Ambler) β-lactamase (*5*). Recently a genetic knockout of the *blaC*-encoded β-lactamase showed that strains lacking this enzyme were more sensitive to β-lactams (*6*). This suggested that the chemical recapitulation of the genetic knockout could similarly resensitize the organism to existing β-lactam antibiotics.

We recently cloned and expressed the *M. tuberculosis blaC* gene and reported a detailed enzymatic characterization (*7*). BlaC exhibits an exceptionally broad substrate specificity, hydrolyzing penicillins at nearly the diffusion-limited rate, all classes of cephalosporins, and, unexpectedly for a class A extended-spectrum β-lactamase, imipenem and meropenem, both carbapenems. Equally unexpected, the enzyme was only transiently inhibited by the β-lactamase inhibitors sulbactam and tazobactam, penicillanic acid sulfones with potent inhibitory activity against other class A β-lactamases. However, clavulanic acid is the only Food and Drug Administration (FDA)–approved β-lactamase inhibitor that irreversibly inhibits BlaC, suggesting that clavulanic acid may recapitulate the genetic knockout, rendering *M. tuberculosis* susceptible to β-lactam antibiotics.

We have previously shown that meropenem was an extremely slow substrate for *M. tuberculosis* BlaC, being hydrolyzed five orders of magnitude slower than ampicillin. A more detailed investigation of the kinetics of meropenem hydrolysis under near stoichiometric enzyme concentrations revealed a steady-state burst with a magnitude dependent on the concentration of BlaC (Fig. 1A). The reaction of meropenem with the enzyme to form the acyl-enzyme intermediate (acylation half-reaction) is fast relative to hydrolysis of the substrate (deacylation). Extrapolation of the final, linear rate to zero time revealed that enzyme acylation was stoichiometric with meropenem. At a single catalytic enzyme concentration, the linear rates yielded plots typical of Michaelis-Menten kinetics (Fig. 1B), with Michaelis constant $K_m = 3.4 \pm 0.7$ μM and turnover number $k_{cat} = 0.08 \pm 0.01$ min^{-1}. Because of its extremely slow turnover rate, we investigated the possibility that meropenem could act as an inhibitor of BlaC and whether it was possible to trap the covalently acylated form of the enzyme. Meropenem acts as a slow, tight-binding inhibitor of the hydrolysis of the chromogenic β-lactam nitrocefin by BlaC. The time courses of nitrocefin hydrolysis are nonlinear in the presence of meropenem, and an analysis of these data yielded an inhibition constant (K_i) value of 16 ± 2 μM and a K_i* value of 1.1 ± 0.8 μM (fig. S1, A and B). The ability of meropenem to act as an inhibitor of BlaC in addition to being a very poor substrate for BlaC added to its potential as an active partner with clavulanate.

The rapid acylation and slow deacylation of BlaC by meropenem suggested that we could observe the covalently bound species by Fourier transform ion cyclotron resonance (FTICR) mass spectrometry. A freshly prepared solution of

[1]Department of Biochemistry, Albert Einstein College of Medicine, 1300 Morris Park Avenue, Bronx, NY 10461, USA. [2]Tuberculosis Research Section, Laboratory of Clinical Infectious Diseases, National Institute of Allergy and Infectious Diseases, National Institutes of Health, Bethesda, MD 20892, USA.

*To whom correspondence should be addressed. E-mail: blanchar@aecom.yu.edu

BlaC and meropenem displayed a peak corresponding to the mass of the covalently acylated BlaC-meropenem complex [charge/mass (m/z) = 29,167.5] and a second peak whose mass corresponded to the mass of the covalently acylated BlaC-meropenem complex –44 (m/z = 29,123.6) (Fig. 1C). After 7 min of incubation, both these peaks decreased in intensity with the corresponding appearance of the free enzyme. Small-molecule mass spectrometry revealed the presence of two species, one with the expected mass for hydrolyzed meropenem (m/z = 402) and another with a mass 44 mass units smaller (m/z = 358, fig. S2). Hydrolysis of meropenem in 1 N NaOH followed by mass spectrometry revealed only the presence of hydrolyzed meropenem. Together, these experiments suggest that, after β-lactam ring opening, the covalently bound meropenem partitions between direct hydrolysis and enzyme-catalyzed decomposition of the C6 hydroxyethyl substituent, yielding acetaldehyde (m/z = 44). The proposed chemical mechanism is discussed below.

The mass spectrometry results suggested that soaking of crystals of BlaC with meropenem followed by vitrification would trap the meropenem complex at the active site. Crystals of BlaC were prepared as previously described (*8*). Crystals soaked for 90 min with 50 mM meropenem containing 20% glycerol were vitrified and analyzed by x-ray diffraction at the Brookhaven National Laboratory Synchrotron Radiation Source. Crystals were present in the same space group as we previously reported for the BlaC-clavulanate complex, and diffraction data to 1.8 Å resolution were used to solve the structure (final model: R_{work} = 0.152 and R_{free} = 0.192, table S1) with molecular replacement methods and the structure of the BlaC-clavulanate complex (*9*). Clear electron density that was contiguous with the β-hydroxyl side chain of Ser^{70} (Ambler numbering is used throughout for residue identification) was observed in the active site (Fig. 2, A and B). The carbonyl oxygen of the covalent enzyme-meropenem ester is oriented to interact with the main chain amide of Ser^{70} and Thr^{253}, residues comprising the "oxyanion" hole. When compared to the structure of the BlaC-clavulanate complex, a number of active site rearrangements are evident. Most notably, the ε-amino group of Lys^{73} and the Ser^{130} side chain hydroxyl no longer hydrogen-bond to the Ser^{70} ester oxygen. The Lys^{73} ε-amino group and the carboxyl side chain of Glu^{166} interact with the meropenem C8 hydroxyl group, whereas the Ser^{130} side chain hydroxyl group hydrogen bonds to the nitrogen of the pyrroline ring (fig. S3). The pyrroline ring shows a collinear relationship of C6, N1, C2, and C3, requiring that the double bond originally present between C2 and C3 has isomerized, as first proposed by Knowles (*10*). The structure clearly shows that the thioether sulfur atom at the C3 position is in the *S* configuration requiring protonation of the *re* face of the C2-C3 double bond. We thus propose a chemical mechanism for meropenem hydrolysis by BlaC as shown in Fig. 2C. The electron density beyond the thioether sulfur atom is weak and discontinuous, so the modeled configuration of the terminal pyrazole ring is uncertain at this time. Whether double bond isomerization is concerted with β-lactam ring opening is also unclear, although we draw it as concerted (Fig. 2C).

The combination of clavulanate and amoxicillin has previously been shown to inhibit the growth of *M. tuberculosis* strains (*11*). Because amoxicillin is one of the best substrates of BlaC, complete inactivation of BlaC would be required to maintain inhibitory concentrations of the antibiotic. More recently, the addition of clavulanate to susceptible and multidrug-resistant strains of *M. tuberculosis* has been shown to potentiate the effects of all classes of β-lactams (*12*, *13*). We determined the minimum inhibitory concentration (MIC) values of *M. tuberculosis* H37Rv in 7H9 medium at 37°C by penicillins, cephalosporins, and carbapenems in the absence and presence of 2.5 μg ml^{-1} clavulanate. The addition of clavulanate had only a modest effect on the MIC values of ampicillin and amoxicillin but a significant effect on the MIC values of cephalothin, imipenem, and meropenem (table S2). On the basis of the low MIC value of meropenem in the presence of clavulanate (0.32 μg ml^{-1}) and its low rate of hydrolysis by BlaC, we selected this carbapenem for detailed analysis. When various combinations of meropenem and clavulanate were added daily for 5 consecutive days to cultures of *M. tuberculosis* Erdman under aerobic growth conditions, the colony-forming units per milliliter (CFU ml^{-1}) dropped rapidly until complete sterilization was obtained after 9 to 12 days (Fig. 3A). Although the number and identity of the cell wall cross-linking transpeptidase targets of meropenem in *M. tuberculosis* are not known (see below), it is clear that a combination of clavulanate and meropenem rapidly sterilizes actively growing aerobic cultures of *M. tuberculosis*.

An important problem in tuberculosis therapy is the phenotypic drug resistance of populations of organisms that are in a nonreplicative state, termed "persistence" (*14*, *15*). The *M. tuberculosis* L,D-transpeptidase has recently been reported to be a target for carbapenems, and this enzyme is thought to be expressed as the organism enters into the persistent state, with corresponding changes in the nature of peptidoglycan cross-linking (*16*). There are several in vitro models of this state, but the most widely used is the Wayne model (*17*), where organisms that are grown in sealed tubes enter into a viable but nonreplicative (NRP) state after 2 weeks because of consumption of available oxygen. Combinations of clavulanate and meropenem were tested for their ability to sterilize organisms in this state. Drug combinations were added to NRP2 cultures within an anaerobic chamber, and cellular viability was assessed 1 week and 2 weeks later by measuring intracellular adenosine triphosphate (ATP) concentrations as well as CFUs. All clavulanate–β-lactam combinations were effective in reducing viability, but the decrease was more pronounced with the two carbapenems, imipenem and meropenem, than with amoxicillin and cefuroxime (fig. S4). In the case of the clavulanate-meropenem combination, we observed more than a log kill over a 2-week exposure time, comparable to metronidazole, which is shown as a control compound in Fig. 3B (*12*).

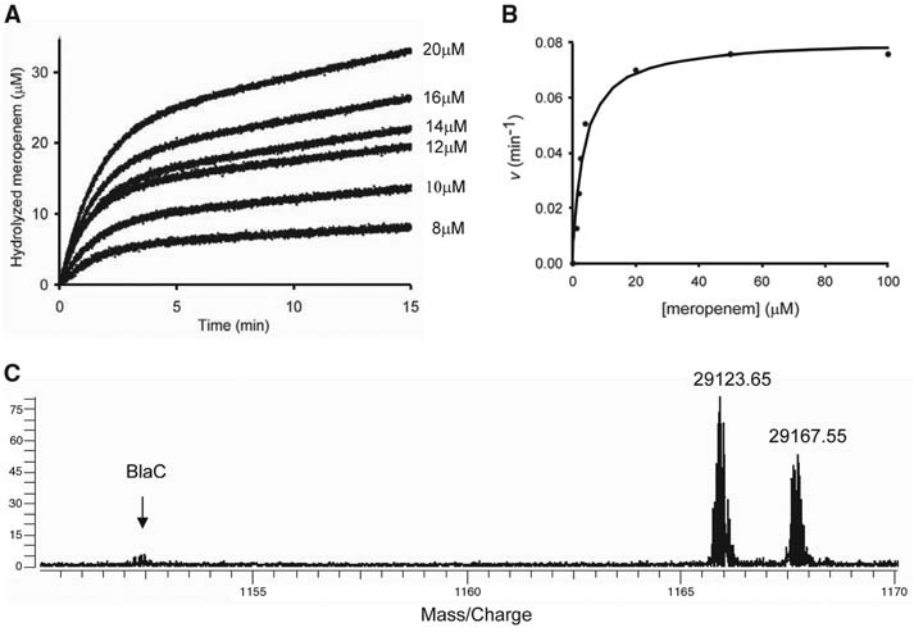

Fig. 1. Kinetics of BlaC with meropenem. (**A**) Time courses of meropenem hydrolysis with various concentrations of BlaC. Enzyme concentrations are reported on the right. (**B**) Michaelis-Menten kinetics of BlaC with meropenem at single enzyme concentration (0.8 μM). (**C**) Mass spectra of enzyme-meropenem species. The 25+ charge state ions are shown. The mass reported for each peak was calculated as described in (*20*) from the two ions with m/z values of 1165.946 and 1167.702.

The combination of clavulanate with β-lactams, especially meropenem, was also tested for the ability to inhibit the growth of extensively drug-resistant (XDR) clinical strains of *M. tuberculosis*. Thirteen clinical isolates exhibiting the XDR phenotype were tested (*18*). Clavulanate was used at a concentration of 2.5 μg ml^{-1}, and the MIC values of these strains for meropenem were determined. The susceptibility of these strains was experimentally indistinguishable from that determined for H37Rv and the Erdman strain, that is, ≤1 μg ml^{-1} (Table 1). In contrast, substantial variability in the MIC values to ampicillin, amoxicillin, cephalothin, and imipenem was observed for these same strains (table S2). The clavulanate-meropenem combination is thus equally effective against both susceptible and XDR strains.

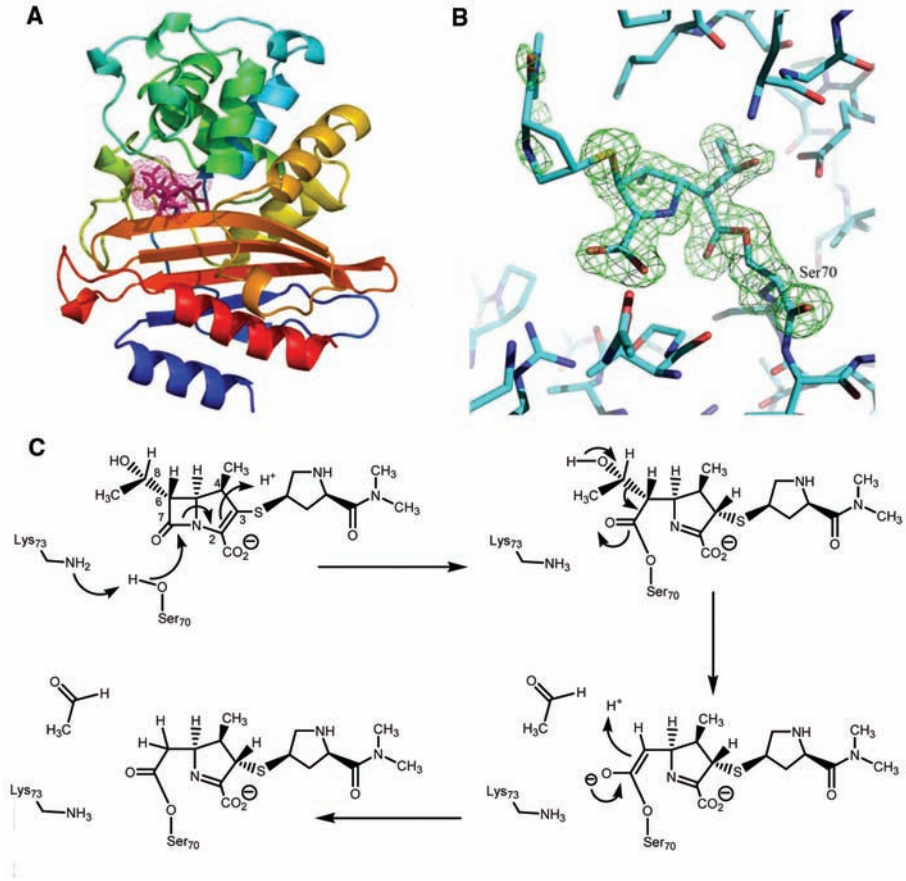

Fig. 2. (**A**) Overall structure of BlaC displayed in rainbow from N term (blue) to the C term (red), with the meropenem adduct displayed as a surface mesh. (**B**) F_o–F_c omit density (green) contoured at 4.0 σ surrounds the covalent meropenem adduct formed at the Ambler active-site residue Ser^{70}. Structure figures were produced using Pymol (www.pymol.org). (**C**) Proposed chemical mechanism for the BlaC-catalyzed reaction with meropenem.

These structural and mechanistic studies of carbapenem interactions with the BlaC β-lactamase have revealed properties of specific β-lactam antibiotics that can be exploited in the treatment of tuberculosis, including the treatment of multidrug- and extensively drug-resistant strains. The structure of the meropenem-inactivated acyl-enzyme, in combination with our mechanistic proposal for its hydrolysis and the structure of the clavulanate-BlaC complex, provides the information necessary to design improved tuberculosis-specific β-lactams that could form longer-lived acyl-enzyme intermediates. Among currently approved β-lactams, however, meropenem is superior on the basis of its poor activity as a substrate for BlaC, ability to transiently inhibit BlaC, and activity against nonreplicating organisms. This activity provides experimental evidence that peptidoglycan remodeling occurs in *M. tuberculosis* in the nonreplicating state, which may be an important determinant of clinical efficacy.

Ten years ago, a report on the early bactericidal activity of amoxicillin-clavulanate in patients with tuberculosis appeared (*19*), but no additional reports have appeared since then. Our studies reveal that clinical strain-to-strain variability is observed with combinations of clavulanate with penicillins, cephalosporins, and imipenem but not with meropenem. The synergism of the clavulanate-meropenem combination and the uniform activity against drug-susceptible, laboratory, and XDR clinical strains suggest this combination could be useful in the treatment of

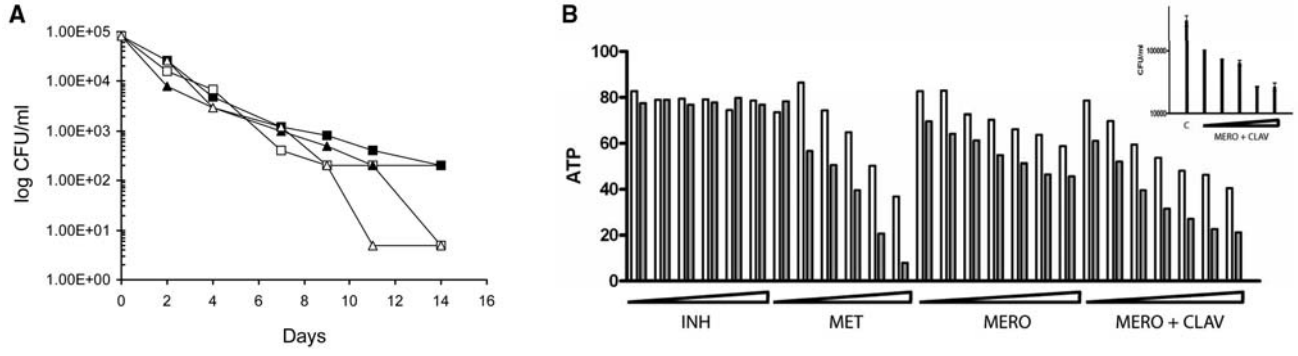

Fig. 3. Killing curves of *M. tuberculosis* after exposure to β-lactams and clavulanate. (**A**) Aerobic growth using the microdilution method. Meropenem and clavulanate were added at 2 μg ml^{-1} + 1 μg ml^{-1} (■), 2 μg ml^{-1} + 2 μg ml^{-1} (□), 4 μg ml^{-1} + 1 μg ml^{-1} (▲), and 4 μg ml^{-1} + 2 μg ml^{-1} (Δ), respectively, for 5 consecutive days. (**B**) Meropenem is cidal for nonreplicating anaerobic *M. tuberculosis*. Hypoxically adapted *M. tuberculosis* H37Rv was treated under anaerobic conditions with twofold dilutions of meropenem (0.19 to 12.5 μg ml^{-1}) in the presence or absence of 2.5 μg ml^{-1} clavulanate. Isoniazid (0.16 to 1.0 μg ml^{-1}) and metronidazole (4.6 to 73 mM) served as negative and positive controls, respectively. Survival was determined by measurement of ATP amounts in surviving bacteria during aerobic outgrowth of 100-fold diluted cells at either 1 week (white bars) or 2 weeks (shaded bars) of treatment or by enumeration of CFUs (inset) after 2 weeks of compound exposure.

Table 1. MIC values for β-lactams in the presence of 2.5 μg ml^{-1} clavulanic acid. The XDR strains were a subset of those previously reported (*18*).

Strain	β-lactam	MIC value (μg ml^{-1})
Erdman	Meropenem	0.5
H37Rv	Amoxicillin	>10
H37Rv	Ampicillin	5.0
H37Rv	Cefotaxime	1.25
H37Rv	Cephalothin	0.94
H37Rv	Imipenem	0.16
H37Rv	Meropenem	0.32
XDR-1	Meropenem	0.94
XDR-2	Meropenem	0.625
XDR-3	Meropenem	0.625
XDR-4	Meropenem	0.625
XDR-5	Meropenem	0.625
XDR-6	Meropenem	0.625
XDR-7	Meropenem	0.625
XDR-8	Meropenem	0.94
XDR-9	Meropenem	1.25
XDR-10	Meropenem	0.47
XDR-11	Meropenem	0.23
XDR-12	Meropenem	0.625
XDR-13	Meropenem	0.32

tuberculosis. Both clavulanate and meropenem are FDA-approved drugs, and both clavulanate and meropenem are sufficiently free of side effects to be approved for pediatric use in children over 3 months old.

References and Notes

1. H. I. Boshoff, C. E. Barry 3rd, *Nat. Rev. Microbiol.* **3**, 70 (2005).
2. N. R. Gandhi *et al.*, *Lancet* **368**, 1575 (2006).
3. A. Fleming, *Br. J. Exp. Pathol.* **10**, 226 (1929).
4. K. Bush, S. Mobashery, *Adv. Exp. Med. Biol.* **456**, 71 (1998).
5. S. T. Cole *et al.*, *Nature* **393**, 537 (1998).
6. A. R. Flores, L. M. Parsons, M. S. Pavelka Jr., *Microbiology* **151**, 521 (2005).
7. J.-E. Hugonnet, J. S. Blanchard, *Biochemistry* **46**, 11998 (2007).
8. F. Wang, C. Cassidy, J. C. Sacchettini, *Antimicrob. Agents Chemother.* **50**, 2762 (2006).
9. L. W. Tremblay, J.-E. Hugonnet, J. S. Blanchard, *Biochemistry* **47**, 5312 (2008).
10. C. J. Easton, J. R. Knowles, *Biochemistry* **21**, 2857 (1982).
11. M. H. Cynamon, G. S. Palmer, *Antimicrob. Agents Chemother.* **24**, 429 (1983).
12. C. Segura, M. Salvado, I. Collado, J. Chaves, A. Coira, *Antimicrob. Agents Chemother.* **42**, 1524 (1998).
13. I. Dincer, A. Ergin, T. Kocagoz, *Int. J. Antimicrob. Agents* **23**, 408 (2004).
14. J. E. Gomez, J. D. McKinney, *Tuberculosis (Edinburgh)* **84**, 29 (2004).
15. Y. Zhang, *Front. Biosci.* **9**, 1136 (2004).
16. M. Lavollay *et al.*, *J. Bacteriol.* **190**, 4360 (2008).
17. L. G. Wayne, L. G. Hayes, *Infect. Immun.* **64**, 2062 (1996).
18. C. Y. Jeon *et al.*, *Clin. Infect. Dis.* **46**, 42 (2008).
19. H. F. Chambers, T. Kocagoz, T. Sipit, J. Turner, P. C. Hopewell, *Clin. Infect. Dis.* **26**, 874 (1998).
20. Materials and methods are available as supporting material on *Science* Online.

21. The authors wish to thank J. Chan and E. Russel for help in the Wayne model studies and H. Xiao for assistance in mass spectrometry. This work was supported partially by the NIH (AI33696 to J.S.B.); in part by the Intramural Research Program of the NIH, National Institute of Allergy and Infectious Diseases; and in part by a grant from the Bill and Melinda Gates Foundation and the Wellcome Trust through the Grand Challenges in Global Health Initiative. A provisional U.S. patent application was filed on 27 May 2008 related to this work. Structure coordinates have been deposited as Protein Data Bank identification code 3DWZ.

Supporting Online Material

www.sciencemag.org/cgi/content/full/323/5918/1215/DC1
Materials and Methods
Figs. S1 to S4
Tables S1 and S2
References

21 October 2008; accepted 6 January 2009
10.1126/science.1167498

Analysis of *Drosophila* Segmentation Network Identifies a JNK Pathway Factor Overexpressed in Kidney Cancer

Jiang Liu,[1,2*] Murad Ghanim,[1,2*†] Lei Xue,[3*] Christopher D. Brown,[1,2] Ivan Iossifov,[1,4‡] Cesar Angeletti,[5] Sujun Hua,[1,2] Nicolas Nègre,[1,2] Michael Ludwig,[1,2,6] Thomas Stricker,[1,2,7] Hikmat A. Al-Ahmadie,[7] Maria Tretiakova,[7] Robert L. Camp,[5] Montse Perera-Alberto,[8] David L. Rimm,[5] Tian Xu,[3] Andrey Rzhetsky,[1,4] Kevin P. White[1,2,6§]

We constructed a large-scale functional network model in *Drosophila melanogaster* built around two key transcription factors involved in the process of embryonic segmentation. Analysis of the model allowed the identification of a new role for the ubiquitin E3 ligase complex factor SPOP. In *Drosophila*, the gene encoding SPOP is a target of segmentation transcription factors. *Drosophila* SPOP mediates degradation of the Jun kinase phosphatase Puckered, thereby inducing tumor necrosis factor (TNF)/Eiger–dependent apoptosis. In humans, we found that SPOP plays a conserved role in TNF-mediated JNK signaling and was highly expressed in 99% of clear cell renal cell carcinomas (RCCs), the most prevalent form of kidney cancer. SPOP expression distinguished histological subtypes of RCC and facilitated identification of clear cell RCC as the primary tumor for metastatic lesions.

Over the last three decades, extensive molecular and genetic analyses have characterized the identity of and interactions between components of the *Drosophila* segmentation process (*1*). Maternal factors distributed in gradients along the anterior-posterior (A-P) axis activate zygotic transcription of gap genes, which encode transcription factors that activate sets of pair-rule genes including the homeobox transcription factors Even-skipped (Eve) and Fushi tarazu (Ftz). These pair-rule proteins then directly regulate segment polarity genes that determine the internal A-P orientation of each segment. Many of the human homologs of these genes and their downstream targets play critical roles in human diseases, especially cancers (*2*, *3*). In an effort to extract new information from the *Drosophila* segmentation network, as well as to mine this network for previously unknown disease-related genes, we built a large-scale predictive network model around Ftz and Eve.

We analyzed gene expression changes between individual wild-type embryos and embryos with null mutations in *ftz* and *eve* (*1*) collected during a developmental time course from 2 hours until 7 hours after egg laying (AEL). By focusing on the effects of Ftz and Eve 2 to 3 hours AEL (early zygotic expression), we found 1310 genes differentially expressed between the *ftz* mutant and wild type, and 1074 genes differentially expressed between the *eve* mutant and wild type (false discovery rate < 0.001; tables S1 and S2).

Using antibodies specific for Ftz or Eve, we performed chromatin immunoprecipitation (ChIP) and mapped genome-wide transcription factor binding in cellular blastoderm embryos 2 hours AEL on custom-designed high-density DNA microarrays (*4*). We found 1286 Ftz- and